Collective Dynamics of Tethered Chains: Breathing Modes

B. Farago
Institut Laue-Langevin, 38042 Grenoble, France

M. Monkenbusch and D. Richter
Institut für Festkörperforschung, Forschungszentrum Jülich, D-5170 Jülich, Germany

J. S. Huang and L. J. Fetters
Exxon Research and Engineering Company, Annandale, New Jersey 08801

A. P. Gast
Department of Chemical Engineering, Stanford University, Stanford, California 94305
(Received 8 March 1993)

Polystyrene(PS)-polyisoprene(PI) diblock copolymers dissolved in *n*-decane aggregate into spherical micelles with a PS core and a corona of tethered PI chains. The PI corona may be considered as a brush on the surface of a sphere or as the outer part of a many-armed polymer star. The thermal density fluctuations of the PI corona have been observed by neutron spin-echo spectroscopy. The peculiar multi-decay time relaxation behavior can be described remarkably well by a model based on an idea of de Gennes for treating the corona as a semidilute polymer solution with varying concentration profile.

PACS numbers: 61.41.+e, 64.60.Ht, 66.10.Cb

When polymer chains are tethered to a surface by one end they form a dense brushlike layer that has attracted considerable interest [1–4]. In addition to their significant practical importance as surface modifiers and colloidal stabilizers, tethered chains represent an interesting constrained structure where osmotic repulsion and elastic energy are in balance. Up until now attention has been focused on predicting [3,4] and measuring [5,6] tethered chain structure and macroscopic forces [2]. Direct information on intermolecular forces may be obtained through a study of the dynamics of tethered chain motion. The connection between constrained chain interactions and collective dynamic response was made some years ago in a simple model proposed by de Gennes [7]. No experimental exploration of these dynamics has yet been undertaken.

Large surface areas of tethered chains can be achieved when an *A-B* diblock copolymer is added to a selective solvent. Under these conditions aggregation analogous to the micellization of surfactants occurs. The outer part of the polymeric micelle containing the soluble blocks has a structure similar to the outer region of a multi-arm polymer star. It may also be viewed as a polymeric brush on a spherical surface [8].

This system allows access to the collective motions within a model layer of tethered chains using neutron spin-echo spectroscopy (NSE). The experimental dynamic structure factors display a distinct time structure comprising an initial fast decay and a slow long time tail. The results agree remarkably well with predictions based on de Gennes' model.

The diblock copolymer studied in this work contains a perdeuterated polystyrene (PS) block and a protonated polyisoprene (PI) block, both obtained via anionic polymerization [9]. The molecular weights of the two blocks measured by size exclusion chromatography are 10000 and 7500 g/mol ($M_W/M_N < 1.03$), respectively. *n*-decane and perdeuterated *n*-decane are the selective solvents readily dissolving the polyisoprene, but not polystyrene.

The aggregate molecular weight of the polymer micelles was determined from low-angle laser-light scattering yielding 2.1×10^6 g/mol and an aggregation number of 120 chains/micelle. From small-angle neutron scattering (SANS) an inner PS core radius of 80 Å was found. At a polymer concentration of 0.25% we determined the hydrodynamic radius by dynamic light scattering to $R_H = 150.5$ Å. The concentration of *A-B* molecules outside micellar aggregates is vanishingly small.

The neutron scattering data in this study were obtained from a 2% PS/PI solution in deuterated decane so that the scattering length density of the PS core was matched to the solvent (shell contrast). Small-angle scattering experiments were carried out using the D17 small-angle camera at the ILL in Grenoble. Standard procedures were followed to correct and normalize the scattering to absolute units (cm^{-1}) [10]. Figure 1 presents typical results. They are characterized by a sharp first minimum followed by a well developed second maximum, indicating a narrow aggregate molecular weight distribution.

The dynamics of the PS/PI micellar corona was investigated by neutron spin-echo spectroscopy. The spin-echo method measures the normalized intermediate dynamic structure factor $I(Q,t)/I(Q,0)$ directly. Unlike usual quasielastic-scattering experiments performed in ω space, the resolution correction in the (Fourier) time domain implies only a division and not a deconvolution of the reference measurement [11] allowing model-independent

0031-9007/93/71(7)/1015(4)$06.00

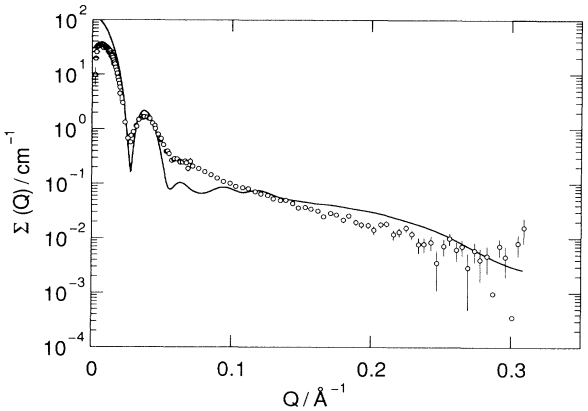

FIG. 1. Log of small-angle neutron scattering intensity (symbols) compared to $I(Q,t=0)$ computed using the fitted parameters. The model calculations did not account for polydispersity and neglect the intermicellar structure factor which reduces the intensity at low Q. Note, however, that structure factor contributions are negligible in the Q range of the NSE experiments.

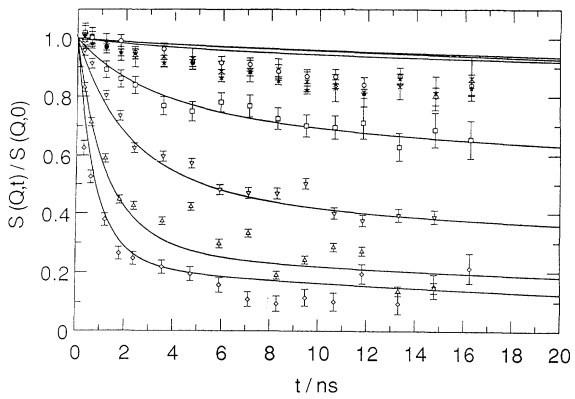

FIG. 2. Measured echo amplitude $I(Q,t)/I(Q,0)$ (symbols) compared to a fit of the model (lines). Different symbols correspond to measurements at $Q=26$ (□), 32 (▽), 38 (*), 51 (×), 64 (◇), 89 (△), and 115 (○) $\times 10^{-3}$ Å^{-1}.

resolution corrections. Experiments were performed on the NSE spectrometer IN11 at the ILL. At a neutron wavelength $\lambda=8.57$ Å and $\Delta\lambda/\lambda=18\%$, we achieved an energy resolution of 20 neV ($1/e$ decay). The experiment accessed a Q range $0.026<Q\leq 0.115$ Å^{-1} over time scales of $0.03\leq t\leq 16.2$ ns. The experiments were carried out at 40 °C with 2 wt% polymer solutions. The data were corrected for background, scattering from the solvent, and resolution. Figure 2 displays the experimental spectra representing the dynamics of the micellar corona. They are characterized by a fast initial decay followed by a slowly relaxing long time tail.

In order to compare with a corresponding linear PI chain, we also studied the dynamics of a $17000 M_W$ ($M_W/M_n=1.05$) chain at 2% monomer concentration in d-decane at 40 °C. Three characteristic spectra ($Q=0.0064$ Å; $Q=0.09$ Å^{-1}; $Q=0.115$ Å^{-1}) are displayed in Fig. 3. The dynamic response from linear PI chains in dilute solution which is governed by the hydrodynamic interaction between chain segments (Zimm model [12]) is completely different from that of the PI chains within the corona. While the relaxation of dilute chains can be well described by the dynamic structure factor for the Zimm model [13] (solid lines in Fig. 3), the qualitative difference of the spectra for corona relaxation indicates a different physical origin for this process.

According to de Gennes [7] the dynamics of an adsorbed polymer layer, having a density which lies in the semidilute solution regime, is determined by the balance of a restoring force due to the osmotic pressure gradient and a viscous force exerted on the polymer due to the motion of the polymer with respect to the background of solvent. A consequence of the semidilute regime is that the osmotic compressibility E and the viscous force coefficient η/ξ^2 depend only on the correlation length ξ or blob size, which is a simple function of the local monomer concentration c, $\xi\propto c^{-3/4}$ [14]. In [7] the equation of motion for the local displacement $\mathbf{u}$ is given for the normal or breathing modes of a planar layer and $\mathbf{u}=u_z(z)\hat{\mathbf{e}}_z$

$$\frac{\partial}{\partial z}\left[E(z)\frac{\partial u}{\partial z}\right]=\frac{\eta}{\xi^2}\frac{\partial u}{\partial t}\,, \tag{1}$$

where z is the distance from the surface.

The density profile describing the planar adsorbed homopolymer layer $c(z)\propto z^{-4/3}$ [15] used in [7] is the same as the (radial) profile for a polymer star or the corona of a starlike micelle [6,16,17]. With this $c(z)$ the

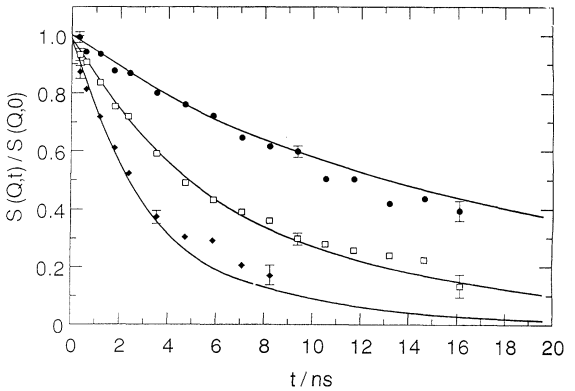

FIG. 3. Dynamic structure factor from a PI chain ($M_W=17000$) in decane 2%. The Q values from above are [$Q=64$(●), 89 (□), and 115 (♦) $\times 10^{-3}$ Å^{-1}]. The solid lines present a fit with the dynamic structure factor for Zimm dynamics [13]. Possible effects of translational diffusion are neglected. The value for the characteristic Zimm constant $T/\eta[K/cP]=356$ agrees within the usual margin [19] with the expected value of 425.

scaling relations for the semidilute solution yield $\xi \propto z$ and $E(z) \propto kT/z^3$. The solutions of Eq. (1) have a simple exponential time decay

$$u(t) = u_n(z)\exp(-t/\tau_n) . \quad (2)$$

Inserting Eq. (2) into Eq. (1) and observing the boundary conditions $[u(z_0)=0$ and $u'(z_{\max})=0]$ yields a Sturm-Liouville boundary value problem with eigenvalues, $1/\tau_n$, and eigenmode functions, $u_n(z)$, for the displacement. Numerical solution [18] yields a spectrum $1/\tau_n = (A+nB)^2$, $n=0,1\ldots$. For typical parameters the times τ_0 and τ_1 differ by about a factor 4; relaxation rates of higher modes increase approximately in a quadratic fashion with the mode number.

Because of the spherical shape of the PS-PI micelles it is necessary to solve the analog of Eq. (1) in spherical coordinates; therefore one has to consider the radial part of

$$\mathrm{grad}[E(r)\mathrm{div}(\mathbf{u})] = \frac{\eta}{\xi^2(r)}\frac{\partial \mathbf{u}}{\partial t} , \quad (3)$$

with $\xi \propto r$ and $E(r) \propto kT/\xi^3$. This results in

$$\frac{\partial}{\partial r}\left(\frac{kT}{r^5}\frac{\partial}{\partial r}y_n\right) - \frac{\eta\lambda_n}{r^4}y_n = 0 , \quad (4)$$

with $y_n = u_{r,n}r^2$, for the radial part of the displacement u_r. The spectrum of the Sturm-Liouville equation (4) has the same shape as that of Eq. (1), $1/\tau_n = \lambda_n = (a+bn)^2$, $n=0,1\ldots$. The intermediate scattering function contribution due to a mode n, $I_n(Q,t)$, depends on the density fluctuation $\delta\rho = \mathrm{div}(c(r)\mathbf{u}_n)$,

$$I_n(Q,t) = \langle\alpha_n^2\rangle |F_T[\mathrm{div}(c(r)\mathbf{u}_n)]|^2 \exp(-t/\tau_n) , \quad (5)$$

where F_T denotes a spatial Fourier transform and $\langle\alpha_n^2\rangle$ is the thermal occupation factor of mode n. In the high-temperature regime $\langle\alpha_n^2\rangle = \frac{1}{2}kT/\Delta F_n$ with ΔF_n the free energy needed to deform the brush according to the mode displacement u_n. The simple exponential time dependence of the problem provides $\Delta F_n \propto \lambda_n$ for normalized u_n.

Equations (1) and (4) can only describe "breathing modes" where all the layers or radial shells move in phase. It is unrealistic to assume that excitations with long wavelengths parallel to the plane or with modulations corresponding to lower spherical harmonics Y_{lm} are suppressed. They contribute to the scattering and therefore must be accounted for. Extension of Eq. (3) to include plane parallel modulations with wave number q modifies the planar eigenvalue problem such that $\lambda_n\eta/kT$ is replaced by $\lambda_n\eta/kT - q^2/z$. The modified spectrum may be approximately described by addition of a term proportional q^2,

$$\lambda_n = (A+Bn)^2 + C_q q^2 . \quad (6)$$

The influence of q on the eigenfunctions, $u_n(z)$, is small. For the spherical problem a solution could not be obtained, but in analogy to Eq. (6)

$$\lambda_{n,l} = (a+bn)^2 + c_l l^2 \quad (7)$$

provides a reasonable approximation. Neglecting nonradial displacements and any l dependence of $u_{r,n}(r)$ the scattering of the "hairy" micelle is

$$I(Q,t) = S(Q) + \sum_{n,l}\left[\langle\alpha_{n,l}^2\rangle 4\pi(2l+1)\left|\int_0^\infty j_l(Qr)[2u_{r,n}cr + (u_{r,n}c)'r^2]dr\right|^2 \exp(-t\lambda_n)\right] , \quad (8)$$

with $\langle\alpha_{n,l}^2\rangle = \gamma kT/\eta\lambda_{n,l}$, where γ subsumes all neglected numerical prefactors. It has to be fitted. $j_l(QR)$ are spherical Bessel functions of order l.

The time scale may be estimated as $\tau_0 = \eta R_b^3/kT\tilde{\lambda}_0 \simeq 20$ ns with R_b equal to the effective brush thickness determining the length scale for which $\tilde{\lambda}_0 \simeq 5$ is a typical value for the lowest eigenvalue of the scaled Eq. (4).

The Brownian motion for the micelles in solution is accounted for by multiplying Eq. (8) with a simple diffusion expression, $\exp(-t/DQ^2)$, with $D = 1.83\times10^{-7}$ cm^2/s from dynamic light scattering (DLS).

Comparison of Eq. (8)—augmented by the micelle center of mass diffusion—with the experimental data shows that this scattering function can explain very well the peculiar time decay curves obtained for higher Q values. However, the low-Q data ($Q \leq 0.038$ Å^{-1}) exhibit a Q-independent extra decay that cannot be reproduced by Eq. (8) because the structure factor of any $u_{r,n}$ eigenmode is virtually zero at these low momentum transfers and the center of mass diffusion is a factor of 4 too slow. Nevertheless remarkably good fits result for higher Q, as illustrated by Fig. 2. The parameters were the inner and outer radii, R_i and R_o, one overall time scale, τ_0, and the ratio of elastic and inelastic scattering, γ. The quality of the fits is virtually insensitive to the maximum $l_{\max}$ to where the sum in Eq. (8) is evaluated as well as to the coefficient, c_l, of the l^2 dependence of λ_n. In the fit of the NSE spectra the geometrical parameters, $R_i = 75$ Å and $R_o = 155$ Å are extremely stable and correspond very well to values obtained from SANS and DLS. The time scale, τ_0, is correlated to changes in $l_{\max}$ and c_l: $c_l/\lambda_{0,0} = 0.1$ yields $\tau_0 = 9.9$ ns; doubling of c_l increases τ_0 to 13 ns, with virtually the same fit quality. The sum in Eq. (8) has been done from $l = 0\ldots12$ and $n = 0\ldots5$, respectively.

A comparison of the small-angle data with $I(Q,t=0)$ as computed using the above micellar dimensions is shown in Fig. 1. The intensity beyond the shell structure peak at 0.035 Å contains significant contributions from the time-dependent density fluctuations. Comparison of the neutron data with the computed intensity shows some intensity deficiency up to $Q < 0.1$ Å; at larger Q the com-

putation yields excess intensity, stemming from high-l fluctuations. The latter observation may be a hint that the high-l modes are more suppressed than imposed by the l^2 dependence of the mode energy.

The salient features of the dynamics of a starlike brush can be described by a simplified model with two important limitations: (1) The viscoelastic response of the brushlike layer is represented solely by an isotropic compressibility; any anisotropy and any shear modulus have been neglected. (2) As a result of technical difficulties the solution of the equation of motion has been restricted to the radial part and is exact only for the breathing mode. Modes proportional to higher spherical harmonics have been incorporated with their radial contributions expressed by $u_{r,n}Y_{lm}$ [Eq. (8)]. Obviously this crude treatment explains the multi-time-constant decays of $I(Q,t)$ for larger Q and the resulting time scale τ_0 is comparable to the predicted estimate. But it fails to give a natural description of the extra decay at small Q values. The reason for the insufficient inelastic intensity produced by the model at small momentum transfers lies in the fact that modes restricted to $u_r \neq 0$ can only produce density redistributions along a radial beam within the brush shell. The maximum extension of possible "density dipoles" is about half the brush thickness, suggesting significant contributions of the corresponding modes only above about $Q \simeq \pi/(2\times 40\ \text{Å}) = 0.04\ \text{Å}^{-1}$. On the other hand it is clear that there should be additional modes with primary displacements parallel to the brush surface that lead to a redistribution of density within the sphere, e.g., from equator to the poles. Such a redistribution proportional to Y_{lm} leads to scattering intensity proportional to $j_1^2(QR_{\text{eff}})$ with $R_{\text{eff}} = 100...150$ Å, yielding substantial contributions for $Q \geq 0.01\ \text{Å}^{-1}$.

The intensity differences between SANS and theoretical predictions have already partly been discussed. At low Q the reduced experimental intensity most likely is related to the influence of an intermicellar structure factor resulting from the repulsion of the aggregates. The missing intensity beyond the second peak in the form factor may result from the polymeric structure inside the concentration blobs, neglected in the above continuum model. At Q values larger than the inverse blob diameter the corresponding form factors will increase the scattering above that of a homogeneous density distribution. Concerning the dynamics such a mechanism will fold the Zimm dynamics onto the relaxation spectra; since it is significantly slower it will not alter the results significantly.

In summary, we have presented NSE experiments on the dynamics of a polymer brush. The essential experimental features may be explained in terms of a continuum model based on a spatially inhomogeneous osmotic compressibility, originally proposed by de Gennes. In order to elucidate the basic physics we have restricted ourselves from adding additional facets which may have improved quantitative agreement but would have masked the nature of the underlying process.

More detailed experiments with planar brushes obtained from *A-B* block copolymers, where the *A* blocks crystallize in the form of platelets, are planned to give a more detailed view of polymer brush dynamics.

[1] A. Halperin, M. Tirrell, and T. P. Lodge, Adv. Polym. Sci. **100**, 31 (1992).

[2] S. S. Patel and M. V. Tirrell, Annu. Rev. Phys. Chem. **40**, 597 (1989).

[3] S. T. Milner, Science **251**, 905 (1991).

[4] S. T. Milner, T. A. Witten, and M. Cates, Macromolecules **21**, 2610 (1988).

[5] K. A. Cogan and A. P. Gast, Macromolecules **23**, 745 (1990).

[6] K. A. Cogan, A. P. Gast, and M. Capel, Macromolecules **24**, 6512 (1991).

[7] P. G. de Gennes, C. R. Acad. Sci. Paris Ser. II **302**, 765 (1986).

[8] B. R. M. Gallot, Adv. Polym. Sci. **29**, 85 (1987).

[9] M. Morton and L. J. Fetters, Rubber Chem. Technol. **48**, 359 (1975).

[10] A. Zirkel, D. Richter, W. Pyckhout-Hintzen, and L. J. Fetters, Macromolecules **25**, 954 (1992).

[11] F. Mezei, *Neutron Spin-Echo* (Springer-Verlag, Heidelberg, 1980).

[12] B. H. Zimm, J. Chem. Phys. **24**, 269 (1956).

[13] E. Dubois-Violette and P. G. de Gennes, Physics (Long Island City, N.Y.) **3**, 181 (1967).

[14] P. G. de Gennes, *Scaling Concepts in Polymer Physics* (Cornell Univ. Press, Ithaca, 1979).

[15] E. Bouchaud, L. Auvray, J. P. Cotton, M. Daoud, B. Farnoux, and G. Jannink, Prog. Surf. Sci. **27**, 5 (1988).

[16] M. Daoud and J. P. Cotton, J. Phys. (Paris) **43**, 531 (1982).

[17] D. Richter, B. Farago, L. J. Fetters, J. S. Huang, and B. Ewen, Macromolecules **23**, 1845 (1990).

[18] Using routine D02KEF from the NAG FORTRAN subroutine library.

[19] D. Richter, in *Structure and Dynamics of Strongly Interacting Colloids and Supramolecular Aggregates in Solutions,* NATO ASI Ser. Vol. 369 (Kluwer Academic, Dordrecht, 1992), p. 111.